ISSN 1560-0904, Polymer Science, Series B, 2019, Vol. 61, No. 6, pp. 753–761. © Pleiades Publishing, Ltd., 2019.

SYNTHESIS

Cyclic Polymer of *N*-Vinylpyrrolidone via ATRP Protocol: Kinetic Study and Concentration Effect of Polymer on Click Chemistry in Solution

Vivek Mishra[a,b,*] and Rajesh Kumar[c]

[a]*Green Chemistry Network Centre, Department of Chemistry, University of Delhi, Delhi, 110007 India*
[b]*Green Process Material Research Group, Korea Institute of Industrial Technology, Chungcheongnam-do, 331-822 Republic of Korea*
[c]*Organic Polymer Chemistry Laboratory, Department of Chemistry, Institute of Science, Banaras Hindu University, Varanasi, UP-221005 India*
**e-mail: vivekbhuchem@gmail.com*

Received April 29, 2019; revised July 17, 2019; accepted August 8, 2019

Abstract—We hereby report the synthesis of a well-defined cyclic poly(*N*-vinylpyrrolidone) using propargyl-2-bromoisobutyrate as an ATRP initiator and NaN_3 followed by the click reaction of alkynyl and azide groups. The decrease of polymer concentration is favorable for cyclization reaction, while the increase of polymer concentration leads to condensation reaction.

DOI: 10.1134/S1560090419060095

INTRODUCTION

The polymers obtained by ATRP contain a functional hand of the initiator on one chain-end and the halide group on the other chain-end. This illustrative makes ATRP remarkably helpful for fabricating different end-functionalized polymers because the halogen atom can be easily transformed into other functional groups using simple standard organic procedure like nucleophilic substitution reaction [1, 2].

Moreover, click reactions [3–5] have gained a great impact of attention due to their high specificity and nearly quantitative yield in the presence of many functional groups. The better yield under mild reaction conditions and resistance of a wide variety of functional groups makes this technique appropriate for the synthesis of controlled polymers with various topologies for polymer modifications [6–10] in biological and materials sciences [11–13]. Click chemistry has been especially helpful in polymer chemistry [14, 15], where less efficient changes frequently experience the harsh effects of incomplete reactions because of the steric detachment of reactive sites inside the polymer design.

Few methods have been developed to control the polymeric design to tailor a material's property for an explicit application. The cyclization of linear polymer ordinarily endures because of poor yield and contending responses, which requires repetitive purification to isolate pure macrocycles. ATRP is a particularly attractive approach for making macrocyclic polymers because of the ability to modify the terminal end group in reasonable yield [14, 16].

Poly(*N*-vinyl pyrrolidone) (PNVP) is a water-soluble biocompatible polymer [17–22] and has been broadly utilized in pharmaceutics, cosmetics, foods, printing inks, textiles, and a lot more diverse applications [23, 24]. PVP and copolymer of *N*-vinyl-2-pyrrolidone (NVP) have been utilized as an antimicrobial specialist in clinical practice [25] and furthermore as the primary segment of temporary skin covers [26] and wound dressings [27].

Therefore, widespread properties and versatile applications of PNVP prompted us to synthesize it by ATRP at ambient temperature, which is successfully utilized for the highly efficient and well-controlled polymerization. Therefore, control of the polymeric structure [28–30] of cyclized-PNVP would furnish an advance material with enhanced and new properties.

In this manuscript, we want to discuss how the highly diluted conditions incredibly enhanced yields in the cyclization process. This is one of the best techniques to synthesize well-controlled intramolecular cyclization of macromolecules.

EXPERIMENTAL

Reagents

NVP (Aldrich, 99%) was refined on 60°C at 8 mm Hg preceding to the experiments. 2,2'-Bipyridyl (bpy), sodium azide, propargyl alcohol, and 2-bromo isobu-

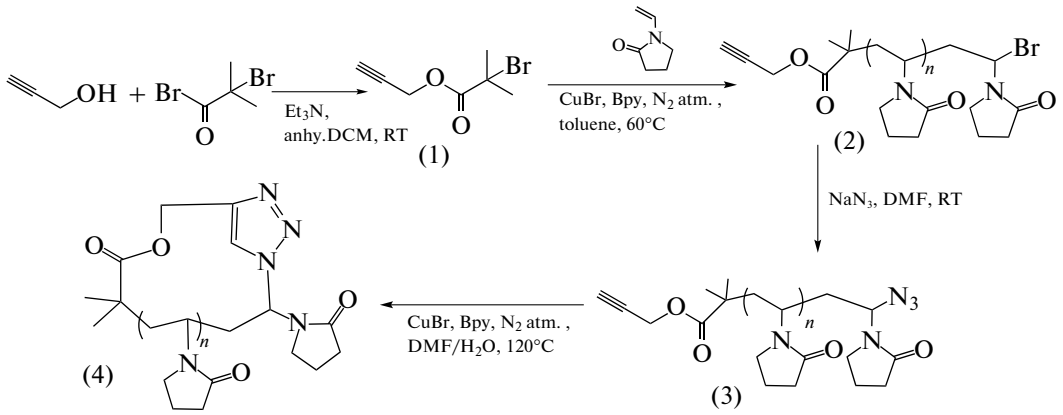

Scheme 1.

tyryl bromide all were purchased from Aldrich with purity 98–99% and utilized in that capacity. Cu(I)Br (Aldrich, 99%) was washed with glacial acetic acid so as to evacuate any soluble oxidized species, filtered, washed with ethanol, and dried. Toluene (Merck, 99.9%) was refluxed under nitrogen over calcium hydride, then distilled and stored over activated molecular sieves under a nitrogen atmosphere. Other liquid reagents and solvents were deoxygenated by purging nitrogen gas prior to use. An azeotropic mixture of DMF with benzene was made and distilled. Anhydrous dichloromethane (DCM) and triethylamine were dried by calcium hydride and distilled prior to use.

Instrumentation

^{1}H NMR spectra were recorded on a JEOL AL300 FTNMR (300 MHz) at ambient temperature in $CDCl_3$ using tetramethylsilane or residual solvent peak as internal standard. The FTIR spectra of the samples in the form of KBr pellets were recorded by a Varian Excalibur 3100 (Palo Alto, CA). The UV–visible spectra were recorded in toluene on PerkinElmer–Lambda 35 UV–Vis Spectrophotometer at 25°C. Molar mass distribution of polymers was performed at 40°C on a Polymer Laboratories PL GPC-220 using THF as an eluent. Molar masses and dispersity $Đ$ were calculated according narrow dispersed PMMA standards.

Syntheses

The general route of the synthesis is given on the Scheme 1.

Propargyl Isobutyryl Bromide (PIBB) Initiator (1)

In 10 mL of anhydrous DCM, propargyl alcohol (0.58 mL, 10 mmol) and triethylamine (1.7 mL, 12 mmol) were taken in an ice-water bath, following with dropwise addition of 2-bromoisobutyryl bromide (1.5 mL, 12 mmol) in 4 mL of DCM. The reaction was quite exothermic and a white precipitate was observed during addition. After stirring overnight at room temperature, the reaction mixture was filtered and the filtrate was concentrated under reduced pressure and then purified by column chromatography using DCM as the eluent. A colorless liquid was obtained (yield 70%). The ^{1}H NMR analysis of the obtained product was consistent with the reported by Matyjaszewski et al. [15] and confirmed the successful synthesis of PIBB.

^{1}H NMR (300 MHz, $CDCl_3$, δ_H, ppm): 4.77(2H, d, CH_2O), 2.51 (1H, t, C≡CH), and 1.96 (6H, s, $(CH_3)_2C$). FTIR spectrum (neat liquid, KBr, cm^{-1}): 3296 ($\nu_{\equiv C-H}$), 2131 ($\nu_{C\equiv C}$), and 1741 ($\nu_{C=O}$). UV/Vis (Toluene): λ_{max} (ε) = 310 nm (1763 M^{-1} cm^{-1}).

Alkynyl-PNVP-Br (2)

In three-neck flask, CuBr (15.6 mg, 0.11 mmol), and bpy (34.4 mg, 0.22 mmol) were added and thoroughly purged with purified nitrogen gas. Deoxygenated distilled NVP (0.37 mL, 3.2 mmol) and PIBB (22.45 mg, 0.11 mmol) in deoxygenated toluene (0.37 mL) was transferred by N_2-purged syringes (10 μL/5 s) to the three-neck flask and four freeze pump thaw cycles were performed to remove oxygen from the reaction. The sealed flask was placed in the oil bath at 60°C. At desired timed intervals, samples were collected. The progress of the reaction was followed by GPC and NMR analysis. The alkynyl-PNVP-Br (2) was precipitated in an excess of diethyl ether and purified by passing it through a short alumina column to remove Cu(II)/bpy complex. The precipitated polymer was collected by centrifugation at 10000 rpm. The isolated polymer was purified by repetitive dissolution in THF and precipitated twice from hexane and dried under vacuum oven at 35°C for 10 h. Monomer conversion was determined gravimetrically and by ^{1}H NMR comparing the integrated peak area of residual vinyl signals at 4.31–4.42 (2H) ppm and 6.99 (1H) ppm of the monomer with that of the

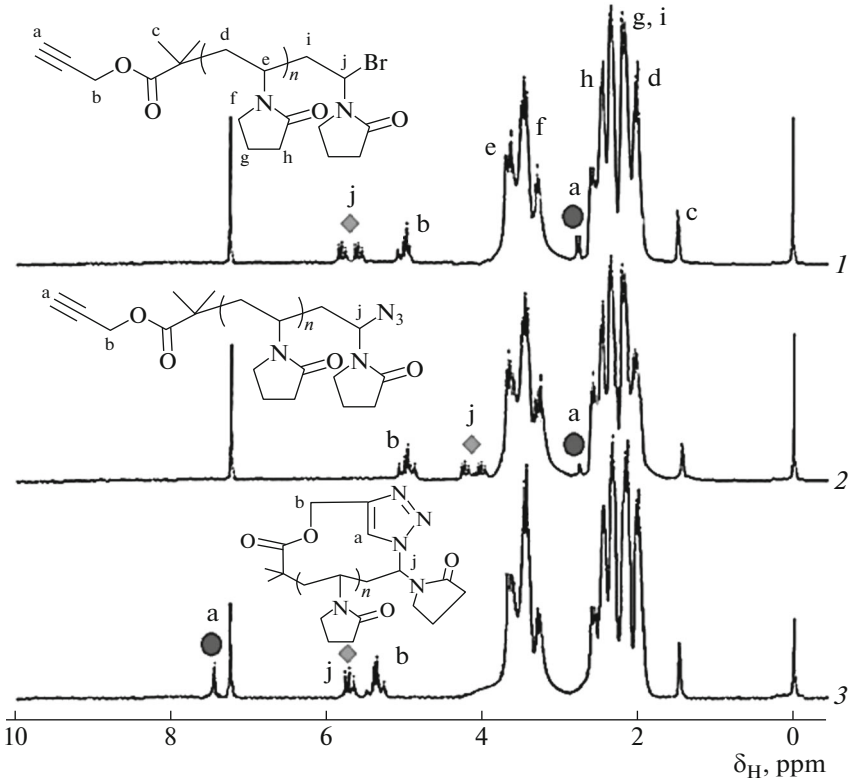

Fig. 1. ^{1}H NMR spectra of (*1*) alkynyl-PNVP-Br, (*2*) alkynyl-PNVP-N_3, and (*3*) cyclized-PNVP.

peak at 1.99–2.04 (2H) ppm and 3.45–3.49 (1H) ppm of the corresponding polymer (Fig. 1).

^{1}H NMR (300 MHz, $CDCl_3$, δ_H, ppm): 5.59–5.79 ($-CH_2-CH-$(pyrrolidone)$-Br$), 4.75–5.09 ($CH\equiv C-CH_2O$), 3.45–3.49 (b, $-N-CH-$), 3.33–3.43 (b, $-N-CH_2-$), 2.68–2.77 ($CH\equiv C-$), 2.27–2.39 (b, $-N-CO-CH_2-$), 2.12–2.17 (b, $-N-CH_2-CH_2-$), 1.99–2.04 (b, $-O_2C-(CH_3)_2-CH_2-$), 1.40 (s, $(-O_2C-CH_3)_2C-$, 6H) (Fig. 1). IR spectrum (KBr plates, ν, cm^{-1}): 3360 (≡C–H, str.), 1295 (≡C–H, weak bending), 655 (≡C–H, strong, bending), 2130 (C≡C, weak, str.), 1187 (–O–C=O–, str., broad, strong), 1748 (α-keto ester, str.), 2915 ($C-CH_3$, asymm. str.,) 1370 ($C-CH_3$, bending), 1000 (C–C, str. of repeating unit, weak), 1325 (C–N str.), 1630 (N–CO–, str. for cyclic tertiary amide), 605 (C–Br, str.) (Fig. 2). UV–Vis (toluene): λ_{max} = 310 nm (Fig. 3).

Alkynyl-PNVP-N_3 (3)

In a round-bottomed flask, an excess amount of sodium azide (5 : 1 ratio with respect to the bromide) was added together with alkynyl-PNVP-Br (2) (135 mg, 50 mmol according to $M_{n,SEC}$) into 5 mL of DMF for 24 h with stirring. The resultant was treated with 100 mL of Brine and taken out with 5 × 100 mL of DCM. The organic layers were dried over magnesium sulfate and diminished by rotator evaporator. The polymer precipitated in excess methanol, gave a white solid (yield 83%). The alkynyl-PNVP-N_3 was collected by filtration and dried under vacuum.

^{1}H NMR (300 MHz, $CDCl_3$, δ_H, ppm): 4.75–5.09 ($CH\equiv C-CH_2O-$), 3.89–4.04 ($-CH_2-CH-$(pyrrolidone)$-N_3$), 3.45–3.49 (b, $-N-CH-$), 3.33–3.43 (b, $-N-CH_2-$), 2.68–2.77 ($CH\equiv C-$), 2.27–2.39 (b, $-N-CO-CH_2-$), 2.12–2.17 (b, $-N-CH_2-CH_2-$), 1.99–2.04 (b, $-O_2C-(CH_3)_2-CH_2-$), 1.40 (s, $(-O_2C-CH_3)_2C-$, 6H) (Fig. 1). IR spectrum (KBr plates, ν, cm^{-1}): 3350 (≡C–H, str.), 1290 (≡C–H, weak bending), 658 (≡C–H, strong, bending), 2131 (C≡C, weak, str.), 1182 (–O–C=O–, str., broad, strong), 1740 (α-keto ester, str.), 2910 ($C-CH_3$, asymm. str.,) 1375 ($C-CH_3$, bending), 1015 (C–C str. of repeating unit, weak), 1330 (C–N str.), 1630 (N–CO–, str. for cyclic tertiary amide), 2113 ($C-N_3$, str.) (Fig. 2). UV–Vis (toluene): λ_{max} = 320 nm (Fig. 3).

Cyclized-PNVP (4)

100 mL of DMF was taken in a 250 mL round bottom flask and degassed using three freeze pump thaw cycles. CuBr (144.5 mg, 1 mmol) and bpy (313 mg,

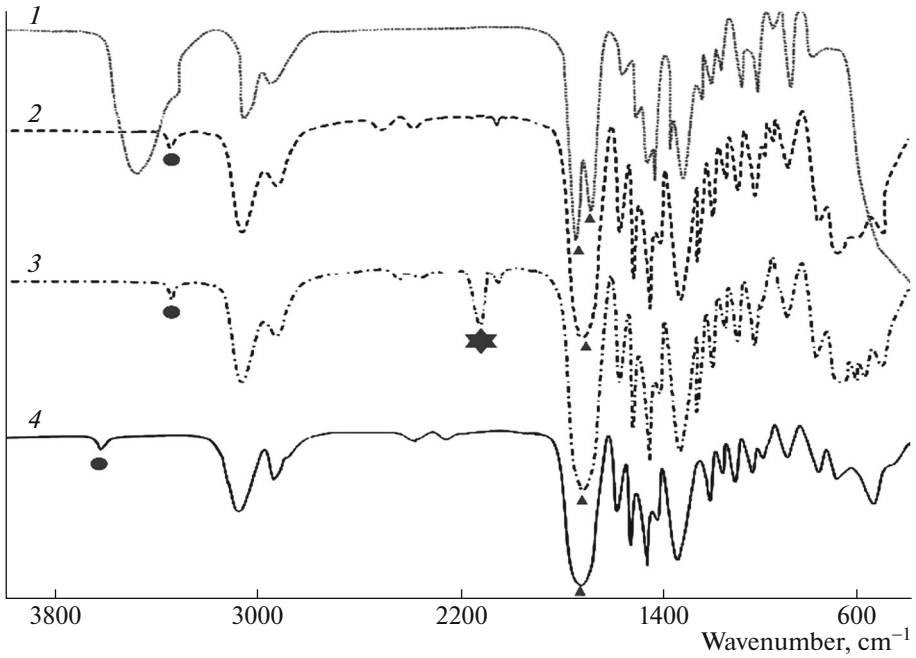

Fig. 2. FTIR spectra of (*1*) NVP, (*2*) alkynyl-PNVP-Br, (*3*) alkynyl-PNVP-N_3, and (*4*) cyclized-PNVP.

2 mmol) were added to the frozen DMF. Then the flask was resealed using rubber septum, evacuated, and refilled with dried N_2 gas. A separate flask containing alkynyl-PNVP-N_3 (3) (50 mg, 0.01 mmol) in 5 mL DMF was degassed through three freeze pump thaw cycles, and afterward, this solution was added to the warm solution of CuBr/bpy at 120°C by a syringe at a feed rate of 0.1 mL/min. Once the addition of the polymer was finished to the catalyst solution, the reaction was allowed to proceed at 120°C for an additional 1 h. Then the reaction was cooled to room temperature and the product was extracted with DCM. The organic layer was washed multiple times with an aqueous saturated solution of $NaHSO_4$, dried over $MgSO_4$, and concentrated in vacuum. The crude product of polymer was precipitated in methanol to give a white solid (yield 75%).

^{1}H NMR (300 MHz, $CDCl_3$, δ_H, ppm): 7.35–7.44 (–N–CH=C–N– of triazole ring), 5.45–5.63 (–CH_2–CH–(pyrrolidone)–N–), 5.13–5.36 (b, –O_2C–$(CH_3)_2$–CH_2–), 3.45–3.49 (b, –N–CH–), 3.32–3.43 (b, –N–CH_2–), 2.27–2.39 (b, –N–CO–CH_2–), 2.12–2.17 (b, –N–CH_2–CH_2–), 1.40 (s, (–O_2C–$CH_3)_2$C–, 6H) (Fig. 1). IR spectrum (KBr plates, ν, cm^{-1}): 3598 (triazine ring, str.), 1175 (–O–C=O–, str., broad, strong), 1720 (α-keto ester, str.), 2920 (C–CH_3, asymm. str.), 1370 (C–CH_3, bending), 1020 (C–C str. of repeating unit, weak), 1335 (C–N str.), 1625 (N–CO–, str. for cyclic tertiary amide) (Fig. 2). UV–Vis (toluene): λ_{max} = 286 nm (Fig. 3).

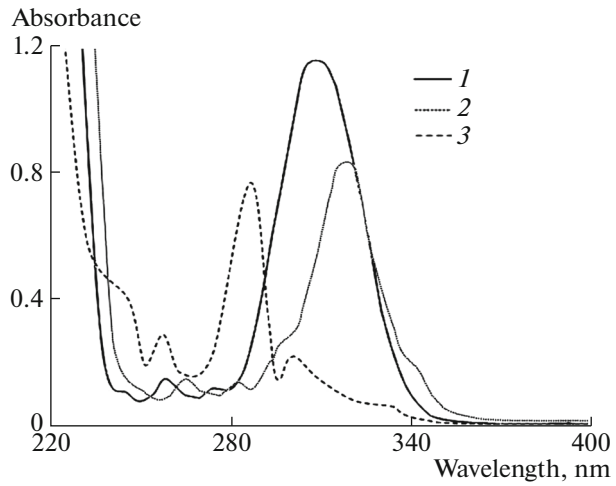

Fig. 3. UV–Vis spectrum of (*1*) alkynyl-PNVP-Br, (*2*) alkynyl-PNVP-N_3 and (*3*) cyclized-PNVP in toluene at the concentration ca. 0.3 g/L.

RESULTS AND DISCUSSION

ATRP of N-Vinypyrrolidone

In order to check the livingness of the polymerization of NVP by ATRP process, the kinetic study was performed at 60°C using PIBB initiator with molar ratio [M] : [I] : [C] : [L] = 30 : 1 : 1 : 2. Figure 4 shows the plot of the monomer conversion and $\ln[M_0]/[M_t]$ versus time. Monomer conversion increases with an approximate 5.6 min induction period. The depen-

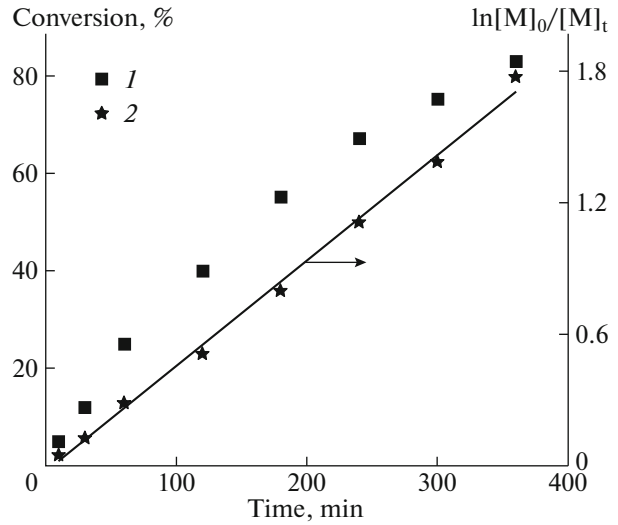

Fig. 4. Dependences of (*1*) monomer conversion and (*2*) $\ln[M_0]/[M_t]$ versus time.

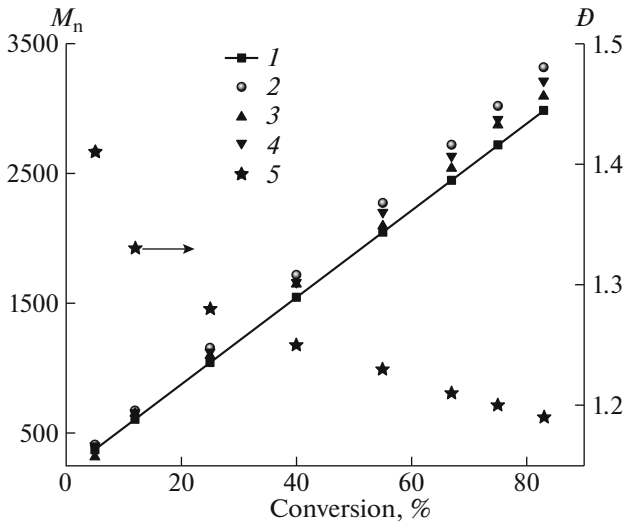

Fig. 5. Dependences of (*1*) $M_{n,\,theory}$, (*2*) $M_{n,\,SEC}$, (*3*) $M_{n,\,NMR}$, (*4*) $M_{n,\,UV}$, and (*5*) $Đ$ versus monomer conversion.

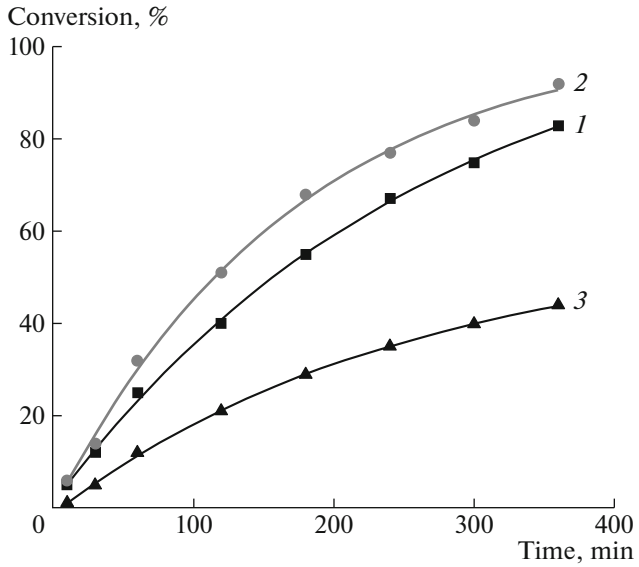

Fig. 6. Dependence of monomer conversion versus polymerization time at various initiator concentrations: $[NVP]_0$: $[PIBB]_0$ = (*1*) 30 : 1, (*2*) 30 : 2, (*3*) 30 : 4.

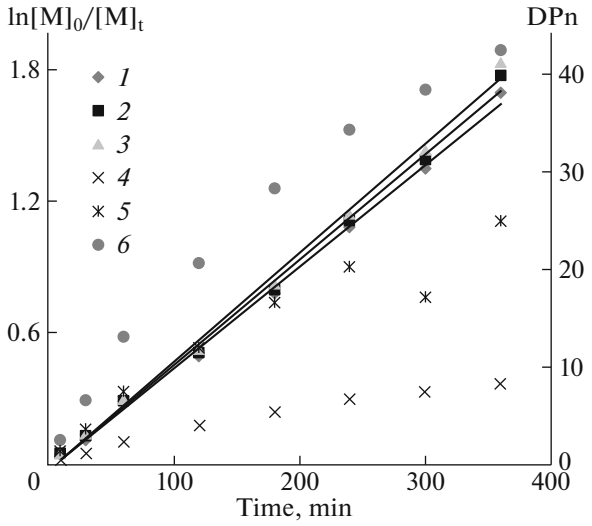

Fig. 7. Dependences of $\ln[M_0]/[M_t]$ from the polymerization time at different ratio [M] : [I] = (*1*) 10 : 1, (*2*) 30 : 1, (*3*) 50 : 1. Dependences of DP_n from the polymerization time at different ratio [M] : [I] = (*4*) 10 : 1, (*5*) 30 : 1, (*6*) 50 : 1.

dence of $\ln[M_0]/[M_t]$ versus time displays a linear tendency, proposing a first-order kinetic character of reaction, which is typical for ATRP. Moreover, the linear increase of M_n versus conversion and low values of molar mass dispersity $Đ$ [31] throughout the polymerization indicated a well-controlled behavior of ATRP (Fig. 5). It is important to notice that the observed M_n values are close to the theoretical values.

According to the data represented in Fig. 6, with the increase of initiator concentration from 30 : 1 to 30 : 2, we have observed an increase in the polymerization rate because of the generation of more free radicals with respect to the monomer. Additionally, an increase in the monomer conversion was observed, but simultaneously the number average molecular weight decreased with increase in the dispersity which is not favorable (Table 1). With further increase in the initiator concentration to 30 : 4, the polymerization rate decreased due to the hindrance in the movement of the free radical initiator and as a result the monomer conversion also diminished. In addition, with the increase in concentration of PIBB, $Đ$ enhanced to 1.43. This recommends the excess initiator concentration moved the ATRP equilibrium towards Cu(II)

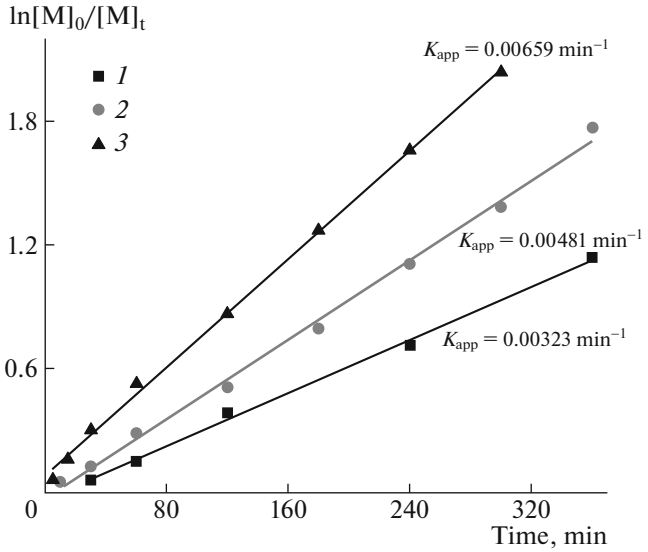

Fig. 8. Dependence of $\ln[M_0]/[M_t]$ versus polymerization time at different temperatures T = (*1*) 323, (*2*) 333, (*3*) 343 K.

species and radicals. On basis of aforementioned grounds, the concentration for [M] : [I] : [C] : [L] was optimized as 30 : 1 : 1 : 2, respectively.

The impact of initial monomer concentration with respect to initiator ($[M]_0 : [I]_0$= 10 : 1, 30 : 1 and 50 : 1) gave the first-order kinetics for each initial monomer concentration with apparent reaction rate coefficient $K_{app} \sim 0.005$ min^{-1} (Fig. 7).

At 10 equivalent of NVP with respect to initiator 90% of monomer conversion is achieved, while at 50 equivalent of NVP only 54% conversion is reached. Simultaneously MWD becomes slightly broader (Table 2). In all the systems molar mass increases throughout polymerization (Fig. 7). Despite the fact that it might be predictable that an increase in initial monomer concentration would affect the activity of the catalyst due to ligand-monomer binding, but the effect was negligible due to the solvation of the monomer in the aqueous medium. This can be clarified by accepting that the diminishing viscosity of a medium with temperature supports the termination of developing chain radicals, and afterward gives a low-molecular-weight polymer.

Table 1. Effect of initiator concentration on ATRP of NVP

[M] : [L] : [C] : [I]	Conversion, %	$M_{n,\,theor}$	$M_{n,\,SEC}$	$Đ$
30 : 2 : 1 : 1	83	3000	3300	1.19
30 : 2 : 1 : 2	92	1330	1480	1.32
30 : 2 : 1 : 4	44	570	700	1.43

Table 2. Effect of monomer concentration on ATRP of NVP

[M] : [L] : [C] : [I]	Conversion, %	$M_{n,\,theor}$	$M_{n,\,SEC}$	$Đ$
10 : 2 : 1 : 1	90	1222	1496	1.21
30 : 2 : 1 : 1	83	2985	3317	1.19
50 : 2 : 1 : 1	54	3234	3593	1.38

The selection of the appropriate concentration of the solvent for ATRP is a very important parameter particularly with the solubility of the catalyst precursor and the relative concentration of the Cu(I)/Cu(II) species. The impact of the polarity of the media in the ATRP of NVP has been explored by means of changing the ratio of toluene/monomer. As shown in Table 3, the polymerization rate diminishes with addition of toluene due to decrease of polarity. However the variety of the polarity of the reaction medium does not play a recognizable impact in the control of the molar mass distribution in the reaction catalyzed by Cu(I)Br/bpy. The nonattendance of the impact of the solvent polarity is in a good concurrence with an inner-sphere electron exchange for both activation and deactivation redox steps [33].

Complexes of a 1 : 1 stoichiometry between Cu(I)Br and bpy are either halogens bridged dimers, bpy-Cu(μ-Br)$_2$Cu-bpy, or 2 : 1 ligand–to–copper cations with a dihalocuprate counter anions, bpy$_2$Cu$^+$CuBr$_2^-$ [34]. To check the impact of ligand concentration 1, 2 and 3 equivalent of bpy as for Cu(I)Br catalyst has been taken (Table 4). The increase of ligand concentration first improves polymerization kinetics and control of molar mass distribution due to the fact that in the less polar media, Br- is destabilized and simultaneously ties a lot more grounded to Cu(I)Br than bpy does, bringing about Cu(bpy)$_2^+$CuBr$_2^-$ species. The further increase of ligand concentration violates control of the process. It is because of the auxiliary bpy (more than 2 : 1) cannot dislodge Br- from the CuBr$_2^-$ anion. The dibromo cuprate anion (CuBr$_2^-$) is inert and does not partake in the ATRP activation process [35, 36]. In this manner, just 50% of the copper species is associated with the activating Cu(I) cation, along these lines, a net change in the transformation is relatively steady.

The influence of the temperature on the kinetics of ATRP of NVP was studied (Fig. 8). Independently from the temperature, polymerization kinetics obeys the first-order law. The rise of the temperature is favorable for the monomer conversion and control of polymerization (Table 5).

Post-Polymerization Modification and Concentration Effect of Polymer on Click Reaction

The SEC traces obtained at different conversions are unimodal and reveal narrow molar mass distribu-

Table 3. Effect of solvent concentration on ATRP of NVP

[NVP]/Toluene	Conversion, %	Time, h	$M_{n,\,theory}$	$M_{n,\,SEC}$	$Đ$
1/0	72	3	2600	2900	2.34
1/1	83	6	3000	3300	1.19
1/2	67	6	2450	2700	1.34

Table 4. Effect of ligand/catalyst ratio on ATRP of NVP

[M] : [L] : [C] : [I]	Conversion, %	Time, h	$M_{n,\,theory}$	$M_{n,\,SEC}$	$Đ$
30 : 1 : 1 : 1	49	12	1850	2050	1.26
30 : 2 : 1 : 1	83	6	3000	3300	1.19
30 : 3 : 1 : 1	84	6	3000	3300	1.33

Table 5. Effect of temperature on ATRP of NVP

Temperature, °C	Conversion, %	Time, h	$M_{n,\,theory}$	$M_{n,\,SEC}$	$Đ$
50	60	12	2200	2900	1.33
60	83	6	3000	3300	1.19
70	87	5	3100	3400	1.09

tion as shown in Fig. 9a. Azido group functionalization of alkynyl-PNVP-Br was confirmed by ^{1}H NMR and FTIR, UV–Vis spectroscopy (Figs. 1–3). In these conditions, the shielding of *j* proton from 5.59–5.79 ($-CH_2-CH-$(pyrrolidone)$-Br$) to 3.89–4.04 ($-CH_2-CH-$(pyrrolidone)$-N_3$) (Fig. 1), and appearance of azide stretching ($\nu_{N=N}$) (as shown in Fig. 2) frequency at 2113 cm^{-1} and change in λ_{max} from 310 to 320 nm in UV–Vis spectrum (as shown in Fig. 3) of azide terminated polymer supports the nucleophilic displacement of bromide group by azide group.

The molar mass distribution has not changed after azidation reaction (Figs. 9b, 9c) due to very low contribution of functional end groups in the average molar mass. Furthermore, the alkynyl-PNVP-N_3 is cyclized by Cu(I)Br/bpy at 120°C in DMF at reflux conditions in N_2 atmosphere in 1 : 2 molar ratio, respectively and at low concentration of alkynyl-PNVP-N_3 equal to 0.01 mmol/L. The macrocyclization resulting in triazole ring formation was confirmed by ^{1}H NMR by appearance of the signals at 5.13–5.36 and 7.43 ppm (Fig. 1). As the SEC data exclude the possibility of condensation, and nearly quantitative formation of the triazole confirms conversion to the macrocycle. The FTIR spectrum of alkynyl-PNVP-N_3 displays a band at 2113 cm^{-1} attributed to the azide stretching. This band has not been detected in the spectrum of the cyclized polymer, bringing further support to the success of the transformation, and the appearance of the band at 3598 cm^{-1} is due to the triazine ring stretching, which also supports the transformation. As is seen on Figs. 9b, 9c, SEC traces of the linear polymers alkynyl-PNVP-Br and alkynyl-PNVP-N_3 almost overlap, while the trace corresponding to the cyclic polymer is moved to longer retention times, i.e. to lower molar masses, due to the discrepancies in hydrodynamic volumes between linear and cyclic polymers. The latter commonly shows higher retention times in SEC analysis.

To prove the suitable conditions for the intramolecular cyclization [37–39], we have also investigated the cyclization of azido-PNVP at three different concentrations of polymers and determined the efficiency of polymer cyclization. We have observed that at higher concentration of azido-PNVP, i.e. 0.2 and 0.5 mmol/L polymer concentrations, the mixture of inter-molecular linear and intra-molecular cyclic-polymer both, with 27, and 65% availability of cyclic polymer products formed. While at low polymer concentration (0.1 mmol/L), a clear intra-molecular cyclized polymer formed. The SEC traces clearly confirmed the formation of cyclic polymers with decrease in the molar concentration (0.5, 0.2, and 0.1 mM) of the azido polymers.

CONCLUSIONS

Thus, the controlled synthesis of PNVP by ATRP at ambient temperature was performed. The polymer-

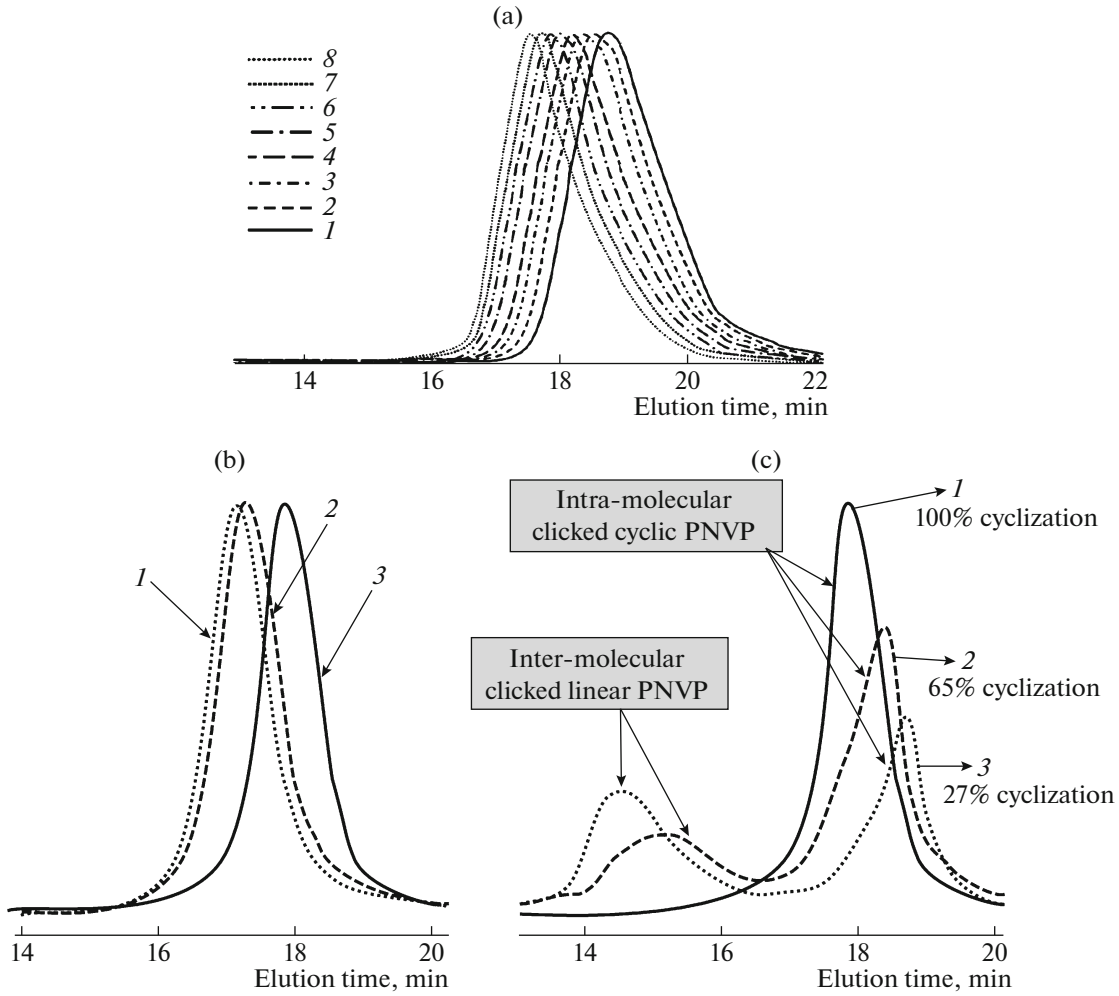

Fig. 9. (a) SEC traces of alkynyl-PNVP-Br at different monomer conversions: (*1*) 5, (*2*) 12, (*3*) 25, (*4*) 40, (*5*) 55, (*6*) 67, (*7*) 75, (*8*) 83. (b) SEC traces of (*1*) PIBB-PNVP-Br, (*2*) PIBB-PNVP-N_3, and (*3*) C-PIBB-NVP. (c) SEC traces of the products of click reaction under various concentrations of polymer: (*1*) 0.1, (*2*) 0.2, and (*3*) 0.3 mM azido-PNVP.

ization of NVP by ATRP was carried out using propargyl 2-bromoisobutyrate as an initiator in toluene. In the range of monomer concentration 1–5 mol/L, the reaction demonstrates the first-order kinetics. The polymer was characterized by narrow dispersity (1.31 to 1.09). Its post-modification with NaN_3 results in the formation of PNVP with terminal alkynyl and azide groups. The cyclization reaction was successfully carried out on alkynyl-PNVP-N_3 with M_n of 3300. We found that the high concentration of polymer (>100 : 1) favored condensation, while dilution favored intra-molecular cyclization. The optimal conditions for click reaction were found and led to the formation of PNVP with a good yield of well-defined ring-shaped cyclic polymer).

ACKNOWLEDGMENTS

The author thanks the Department of Chemistry, BHU, Varanasi (India) and Department of Chemistry, the University of Delhi for providing spectral and analytical facilities and SERB, New Delhi for providing financial support in the form of National PDF.

FUNDING

This work was financially supported by a grant from SERB research Project Supported by the Department of Science and technology, New Delhi in the form of National-PDF (Grant no. PDF/2017/000952).

CONFLICT OF INTEREST

The authors declare that they have no conflict of interest.

REFERENCES

1. L. Yang, H. Sun, Y. Liu, W. Hou, Y. Yang, R. Cai, C. Cui, P. Zhang, X. Pan, X. Li, L. Li, B. S. Sumerlin, and W. Tan, Angew. Chem., Int. Ed. **57**, 17048 (2018).

2. V. Coessens, T. Pintauer, and K. Matyjaszewski, Prog. Polym. Sci. **26**, 337 (2001).
3. H. Sun, C. P. Kabb, M. B. Sims, and B. S. Sumerlin, Prog. Polym. Sci. **89**, 61 (2019).
4. H. C. Kolb, M. Finn, and K. B. Sharpless, Angew. Chem., Int. Ed. **40**, 2004 (2001).
5. Q. Wang, T. R. Chan, R. Hilgraf, V. V. Fokin, K. B. Sharpless, and M. G. Finn, J. Am. Chem. Soc. **125**, 3192 (2003).
6. H. Sun, C. P. Kabb, Y. Dai, M. R. Hill, I. Ghiviriga, A. P. Bapat, and B. S. Sumerlin, Nat. Chem. **9**, 817, (2017).
7. V. Mishra, S.-H. Jung, J. M. Park, H. M. Jeong, and H.-I. Lee, Macromol. Rapid Commun. **35**, 442 (2014).
8. B. S. Sumerlin, N. V. Tsarevsky, G. Louche, R. Y. Lee, and K. Matyjaszewski, Macromolecules **38**, 7540 (2005).
9. Y. Li, J. Yang, and B. C. Benicewicz, J. Polym. Sci., Part A: Polym. Chem. **45**, 4300 (2007).
10. R. Riva, S. Schmeits, C. Jérôme, R. Jérôme, and P. Lecomte, Macromolecules **40**, 796 (2007).
11. J. F. Lutz, Angew. Chem., Int. Ed. **46**, 1018 (2007).
12. X. Jiang, M. C. Lok, and W. E. Hennink, Bioconjugate Chem. **18**, 2077 (2007).
13. W. H. Binder and R. Sachsenhofer, Macromol. Rapid Commun. **28**, 15 (2007).
14. V. Mishra, S.-H. Jung, H. M. Jeong, and H.-I. Lee, Polym. Chem. **5**, 2411 (2014).
15. N. V. Tsarevsky, B. S. Sumerlin, and K. Matyjaszewski, Macromolecules **38**, 3558 (2005).
16. K. Matyjaszewski and J. Xia, Chem. Rev. **101**, 2921 (2001).
17. V. Mishra and R. Kumar, J. Appl. Polym. Sci. **124**, 4475 (2012).
18. V. Mishra and R. Kumar, *Functional Controlled/Living Radical Polymers: Synthesis, Kinetics and Physico-Chemical Properties* (Lambert Acad. Publ., GmbH, Germany, 2013), p. 133.
19. V. Mishra and R. Kumar, J. Appl. Polym. Sci. **128**, 3295 (2013).
20. A. Srivastava, V. Mishra, P. Singh, A. Srivastava, and R. Kumar, J. Therm. Anal. Calorim. **107**, 211 (2012)
21. A. Srivastava, V. Mishra, S. K. Singh, and R. Kumar, e-Polym. **6**, 1 (2009).
22. V. Mishra and R. Kumar, Trends Carbohydr. Res. **4** (3), 1 (2012).
23. V. Mishra and R. Kumar, Carbohydr. Polym. **83**, 1534 (2011).
24. F. Haaf, A. Sanner, and F. Straub, Polym. J. **17**, 143 (1985).
25. L. Nud'ga, V. Petrova, N. Klishevich, L. Litvinova, A. Y. Babenko, and V. Shelegedin, Russ. J. Appl. Chem. **75**, 1678 (2002).
26. M. J. O'Connell, P. Boul, L. M. Ericson, C. Huffman, Y. Wang, E. Haroz, C. Kuper, J. Tour, K. D. Ausman, and R. E. Smalley, Chem. Phys. Lett. **342**, 265 (2001).
27. Y. Nho and K. Park, J. Appl. Polym. Sci. **85**, 1787 (2002).
28. Q. Tang, J. Chen, Y. Zhao, and K. Zhang, Polym. Chem. **6**, 6659 (2015).
29. V. M. Treushnikov, N. V. Frolova, L. L. Pomerantseva, and A. V. Olenik, Polym. Sci. U.S.S.R. **20**, 1371 (1978).
30. S. Honda, T. Yamamoto, and Y. Tezuka, Nat. Commun. **4**, 1574 (2013).
31. R. Gilbert, M. Hess, A. Jenkins, R. Jones, P. Kratochvil, and R. Stepto, Pure Appl. Chem. **81**, 351 (2009).
32. X.-P. Qiu, F. Tanaka, and F. M. Winnik, Macromolecules **40**, 7069 (2007).
33. A. K. Nanda and K. Matyjaszewski, Macromolecules **36**, 599 (2003).
34. X.-S. Wang and S. Armes, Macromolecules **33**, 6640 (2000).
35. K. Matyjaszewski, T. E. Patten, and J. Xia, J. Am. Chem. Soc. **119**, 674 (1997).
36. A. T. Levy, M. M. Olmstead, and T. E. Patten, Inorg. Chem. **39**, 1628 (2000).
37. B. A. Laurent and S. M. Grayson, J. Am. Chem. Soc. **128**, 4238 (2006).
38. D. M. Eugene and S. M. Grayson, Macromolecules **41**, 5082 (2008).
39. D. E. Lonsdale, C. A. Bell, and M. J. Monteiro, Macromolecules **43**, 3331 (2010).